

Article

Evaluation of Field Germination of Soybean Breeding Crops Using Multispectral Data from UAV

Rashid Kurbanov ¹, Veronika Panarina ², Andrey Polukhin ², Yakov Lobachevsky ¹, Natalia Zakharova ¹, Maxim Litvinov ¹, Nazih Y. Rebouh ³, Dmitry E. Kucher ³, Elena Gureeva ⁴, Ekaterina Golovina ², Pavel Yatchuk ², Victoria Rasulova ² and Abdelraouf M. Ali ^{3,5,*}

- ¹ Federal Scientific Agroengineering Center VIM, 1st Institut'skiy proezd 5, 109428 Moscow, Russia; celeba@outlook.com (R.K.); lobachevsky@yandex.ru (Y.L.); smedia@vim.ru (N.Z.); litvvinov.max@yandex.ru (M.L.)
- ² Federal Scientific Center of Legumes and Groat Crops, Molodezhnaya Str. 10/1, Village Streletsky, 302502 Oryol, Russia; ver1183@yandex.ru (V.P.); polukhinogac@yandex.ru (A.P.); kat78010@mail.ru (E.G.); p1a9v8e8l@mail.ru (P.Y.); 567live357@mail.ru (V.R.)
- ³ Department of Environmental Management (RUDN University), 6 Miklukho-Maklaya St, 117198 Moscow, Russia; n.yacer16@outlook.fr (N.Y.R.); kucher_de@pfur.ru (D.E.K.)
- ⁴ Institute of Seed Production and Agrotechnologies Branch of Federal Scientific Agroengineering Center VIM, Parkovaya Str. 1, Podvyazye Village, Ryazan District, 390502 Ryazan, Russia; elenagureeva@bk.ru
- ⁵ National Authority for Remote Sensing and Space Sciences (NARSS), Al-Nozha Al-Gedida, Cairo P.O. Box 1564, Egypt
- * Correspondence: raouf.shoker@narss.sci.eg

Abstract: The use of multispectral aerial photography data contributes to the study of soybean plants by obtaining objective data. The evaluation of field germination of soybean crops was carried out using multispectral data (MSD). The purpose of this study was to develop ranges of field germination of soybean plants according to multispectral survey data from an unmanned aerial vehicle (UAV) for three years (2020, 2021, and 2022). As part of the ground-based research, the number of plants that sprang up per unit area was calculated and expressed as a percentage of the seeds sown. A DJI Matrice 200 Series v2 unmanned aerial vehicle and a MicaSense Altum multispectral camera were used for multispectral aerial photography. The correlation between ground-based and multispectral data was 0.70–0.75. The ranges of field germination of soybean breeding crops, as well as the vegetation indices (VIs) normalized difference vegetation index (NDVI), normalized difference red edge index (NDRE), and chlorophyll index green (CI_{Green}) were calculated according to Sturges' rule. The accuracy of the obtained ranges was estimated using the mean absolute percentage error (MAPE). The MAPE values did not exceed 10% for the ranges of the NDVI and CI_{Green} vegetation indices, and were no more than 18% for the NDRE index. The final values of the MAPE for the three years did not exceed 10%. The developed software for the automatic evaluation of the germination of soybean crops contributed to the assessment of the germination level of soybean breeding crops using multispectral aerial photography data. The software considers data of the three vegetation indices and calculated ranges, and creates an overview layer to visualize the germination level of the breeding plots. The developed method contributes to the determination of field germination for numerous breeding plots and speeds up the process of breeding new varieties.

Keywords: digital agriculture; remote sensing; unmanned aerial vehicle; multispectral data; soybean; breeding



Citation: Kurbanov, R.; Panarina, V.; Polukhin, A.; Lobachevsky, Y.; Zakharova, N.; Litvinov, M.; Rebouh, N.Y.; Kucher, D.E.; Gureeva, E.; Golovina, E.; et al. Evaluation of Field Germination of Soybean Breeding Crops Using Multispectral Data from UAV. *Agronomy* **2023**, *13*, 1348. <https://doi.org/10.3390/agronomy13051348>

Academic Editors: Maofang Gao and Mohamed A.E. AbdelRahman

Received: 7 April 2023

Revised: 5 May 2023

Accepted: 8 May 2023

Published: 11 May 2023



Copyright: © 2023 by the authors. Licensee MDPI, Basel, Switzerland. This article is an open access article distributed under the terms and conditions of the Creative Commons Attribution (CC BY) license (<https://creativecommons.org/licenses/by/4.0/>).

1. Introduction

Increasing the acreage under soybeans is a solution to the problem of the shortage of high-grade vegetable protein in the Russian Federation. Soybeans are actively spreading in the northwest direction, and until now the main centers of their cultivation were the Far

Eastern, North Caucasian, and Central Federal Districts [1]. Changing climatic conditions also require the search and creation of adapted varieties [2]. Therefore, it is necessary to study the plants of such varieties during the phenology stages, namely, stage I (seed germination) and stage II (germination), which are especially important since the further development of the plant depends on them [3].

To fully realize the genetic potential of cultivated varieties of agricultural crops, it is important to ensure the high quality of their seeds [4]. For this purpose, in accordance with the Federal Law “On Seed Production” [5], seeds intended for sowing were subjected to inspection for varietal and sowing qualities during varietal and seed control. High-quality seeds have high indicators of germination energy, laboratory germination, and growth strength, which ensures the production of friendly seedlings and high field germination. If the seeds have low quality indicators, there is an increase in sparse crops and the formation of plants with low productivity.

There are many factors affecting the germination energy and field germination of seeds, such as soil temperature, soil granulometric composition, the depth and uniformity of seed embedding in the soil, the presence of moisture, the appearance of disease, and others. The soybean is a thermophilic culture by its biology; the minimum temperature for seed germination is +8 to +10 °C, with +10 °C being more favorable, and the temperature range of +12 to +14 °C contributes to the appearance of friendly seedlings [6,7]. The increase in field germination leads to a properly selected depth for sowing seeds and their uniform embedding in the soil [8]. A large depth of seed deepening leads to an elongation of the germination period and there is a risk of soil infection. Conversely, insufficient deepening leads to uneven seedlings and the production of weakened plants. An essential condition for the emergence of seedlings is the presence and amount of moisture in the soil. Seeds require at least 130–160% of their weight in water to germinate [7,9]. Weather conditions directly affect the amount of moisture in the soil. Prolonged rains or periods of drought adversely affect germination. Thus, field germination is a complex indicator that includes the quality of seeds, the level of agricultural technology, soil composition, weather conditions, etc. Due to the variety of factors affecting the field germination of soybean plants, researchers did not identify a relationship between laboratory germination and field germination [10,11].

Field germination is estimated by counting the germinated plants per unit area and expressing it as a percentage of the sown seeds. However, this method requires not only certain physical costs but also time. With the development of modern digital technologies, it has become possible to search for new methods to assess field germination [12,13].

Remote sensing methods are used to map vegetation in the agricultural sector [14]. In recent years, unmanned aerial vehicles (UAVs) have attracted considerable interest in solving problems in the breeding process [15–17]. In particular, UAVs with optical suspension equipment have become useful tools in the evaluation of breeding plots [18–20]. The use of UAVs makes it possible to study breeding crops and obtain objective data on several signs and physiological qualities of studied crops [21–23]. In the study of soybean plants, various vegetation indices are used [24–26] for phenotyping [27], yield forecasting [28–30], flood stress assessment [31], drought [32], detection of weeds [33], and fertilizing [34]. The issue of assessing the field germination of soybean crops using multispectral data was not sufficiently disclosed, and its further study is relevant.

In connection with the above, the purpose of our research was as follows: to develop field germination ranges for breeding soybean plants according to multispectral survey data from an unmanned aerial vehicle.

2. Materials and Methods

2.1. Study Area

In 2020, the study occurred on soybean breeding crops at the Institute of Seed Production and Agrotechnology’s (ISA—branch of the Federal State Budgetary Institution “Federal Scientific Agroengineering Center VIM”), Ryazan region, 54°34′43.1″ N 39°33′6.5″ E. The

total area of the field under study was 1.0 ha. In 2021 and 2022, the research took place in the fields of the Federal State Budgetary Scientific Institution “Federal Scientific Center for Legumes and Cereals” (FGBNU FNC ZBK), Oryol region, 53°0′50.3″ N 35°59′25″ E. The total area of the field under study was 1.72 ha and 2.75 ha in 2021 and 2022, respectively (Figure 1). The study took into account the data of 1460 plots (2020: 126 plots, 2021: 416 plots, and 2022: 918 plots). The study of varieties and varieties according to economically useful characteristics was carried out using the method of small-scale testing, where the sizes and shapes of plots for each stage of selection were determined in accordance with the methodology of B.A. Dospekhov’s field experience [35] and the methodology of the state variety testing of agricultural crops [36]. The plot area in the breeding nursery was 6.75 m² (6.75 × 1.0 m), in the control nursery it was 8.1 m² (5.4 × 1.5 m), and in the nursery for competitive variety testing it was 12.8 m² (8 × 1.6 m). The repetition, depending on the nursery, was three to five times. Plots in the breeding nursery were studied in amounts of 44 units. The number of plots in the control nursery was 698, and in the nursery of the competitive variety test it was 718. A total of 744 plots (2020: 42 plots, 2021: 232 plots, and 2022: 470 plots) were used in the calculation of the range values of field germination (test plots), while 716 plots (2020: 84 plots, 2021: 184 plots, and 2022: 448 plots) were used to assess the accuracy of the obtained results (verification plots).

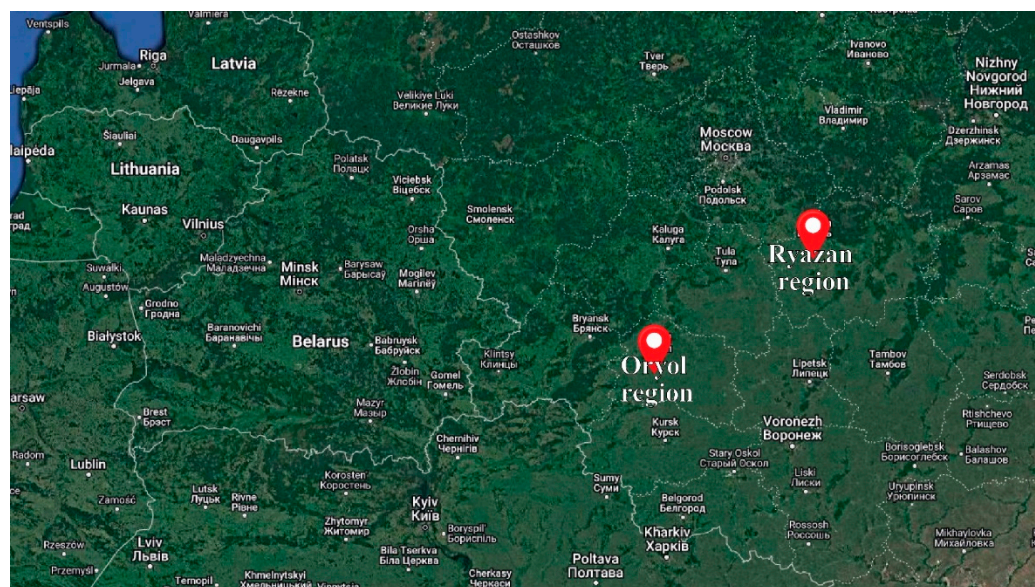


Figure 1. Locations of the study areas.

2.2. Ground Studies

Testing of soybean seeds for sowing included varietal and sowing qualities according to state standard R 52325-2005 [37]. Soybean sowing in 2020 took place in the period from 12 May to 14 May, with wide-row sowing and a row spacing width of 45 cm. On 11 June 2020, in the phase of full seedlings, the density of standing plants was determined. The field germination rate (%) was calculated relative to the number of normal seedlings and the number of germinating seeds sown per unit area (Figure 2a). The number of ascended plants was considered in three middle rows at a length of 0.74 cm.

Soybean seeds were sown in 2021 from 18 May to 20 May, and in 2022 from 24 May to 28 May. The germination assessment experiment was conducted on 13 June 2021 and 14 June 2022, in which plant germination was determined using ground methods, namely, by counting the plants that had sprung up per unit area and expressing them as a percentage of seeds sown. When considering the density of plants, as a guide, we used the methodology of the state variety testing of agricultural crops [36] and the international common list of descriptors for the genus *Glycine Wild* [38]. The width of the row spacing in the soybean

crops was 45 cm, and the number of germinating plants was determined in four rows at a length of 0.55 cm (Figure 2b,c).

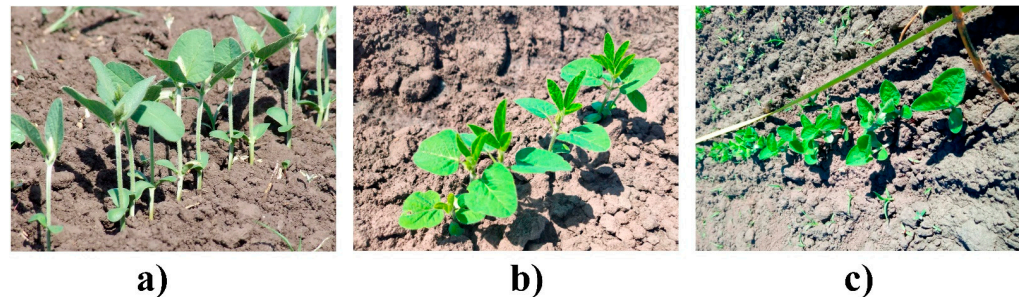


Figure 2. Plots of soybean plants: (a) 11 June 2020; (b) 13 June 2021; (c) 14 June 2022.

2.3. Unmanned Aerial Vehicle Platform and Sensor

In this study, we used an unmanned aerial vehicle (UAV) quadcopter, namely, a DJI Matrice 200 Series v2, with post-processed kinematic (PPK) aerial photography (Figure 3). The quadcopter had two cameras on board: a DJI X4S 20 megapixel RGB camera with a resolution of 5472×3648 , and a MicaSense Altum multispectral camera with a downwelling light sensor (DLS 2). A three-axis suspension attached the DJI X4S camera to the drone. The multispectral camera was installed using a specialized suspension that considers the mutual position of the multispectral camera and the DLS 2, the drone sensors, and the camera power from the UAV board. The MicaSense Altum simultaneously captured images in six channels: blue (B) (475 ± 32 nm), green (G) (560 ± 27 nm), red (R) (668 ± 16 nm), red edge (RE) (717 ± 12 nm), near-infrared (NIR) (842 ± 57 nm), and long wavelength infrared (LWIR) (thermal infrared 8–14 μm). The resolution of the 3.2 MP spectral channels was 2064×1544 and the thermal channel was 160×120 .



Figure 3. Monitoring of soybean crops using a quadcopter DJI Matrice 200 Series v2 in the Oryol region in 2022.

The calibration panel was used before and after the flight according to the recommendations of the camera manufacturer. The DLS 2 was used for irradiance and sun angle measurements, as well as fixing the shooting coordinates of each image. These radiometric calibration tools considered various weather conditions and illumination. Using this method of data calibration, it was possible to analyze time series data and compare them from different years. We used DJI Pilot, a mobile application, for flight planning and implementation.

This UAV is proven to be a reliable platform for the study of agricultural crops, such as winter cereals [39] and grain sorghum [40], as well as for various scientific purposes, for example, the detection and analysis of methane emissions, counting open cotton bolls and

estimating lint yield, and the detection of apple fire blight [41–43]. The drone has a degree of protection of IP43 (protection from dust and moisture) and can fly at wind gusts up to 20 m/s, which is important when working in the field.

Monitoring was carried out on 11 June 2020, 13 June 2021, and 14 June 2022 at a height of 120 m. To obtain high-precision data, a multi-frequency GNSS receiver called EMLID Reach RS2 was used. The connection took place to the base station “OREL” in the Orel region and “RYAZ” in the Ryazan region, located less than 20 km from the aerial photography sites. Ten 50-by-50 ground control points (GCPs) were used to check the accuracy of the data. The GCPs were evenly spaced on the field, considering height differences.

The calculation of flight parameters (altitude, flight speed, and overlap of images) was carried out considering the installation of two cameras on board at the same time. The altitude and flight speed were calculated based on the technical characteristics of the multispectral camera, since it has a lower resolution than the RGB camera. The ground sampling distance (GSD) was selected in accordance with the task set for the overall assessment of the state of small-scale sowing without counting the number of plants on the plot. To assess the general condition of plants, GSD varies from 2.5 to 10 cm/px [44–46]. In our work, GSD was selected up to 6 cm/pixel. Based on the selected GSD, the maximum flight altitude was 120 m. At such a flight altitude, multispectral data of sufficient quality were collected for analysis, and minimal time was spent on flight and photogrammetric data processing.

The flight speed was calculated considering the technical characteristics of the RGB and multispectral cameras according to Formula (1). The transverse overlap for the RGB camera was calculated considering the length of the image of the multispectral camera.

$$V = \frac{b_x \times \frac{(100 - P_x)}{100} \times GSD}{t \times 100} \quad (1)$$

where b_x is the width of the multispectral camera image in pixels; P_x is the longitudinal overlap for a multispectral camera in %; and t is the time taken by the cameras to create and record an image from a single shooting point, s.

2.4. Data Processing

This study used vegetation indices related to the assessment of biomass, NDVI (normalized difference vegetation index); the nitrogen content in plant leaves, NDRE (normalized difference red edge index); and the chlorophyll a and b content in plant leaves, ClGreen (chlorophyll index green). Photogrammetric data processing was carried out in the PIX4Dmapper software (Version 4.8.4). Vegetation indices were calculated using the green, red, red edge, and NIR reflectance bands. For each of the plots, the average values of the vegetation indices (2)–(4) were determined in the PIX4Dfields software (Version 2.3.1).

$$NDVI = \frac{NIR - R}{NIR + R} \quad (2)$$

$$NDRE = \frac{NIR - R}{NIR + R} \quad (3)$$

$$ClGreen = \frac{NIR}{G} - 1 \quad (4)$$

To estimate the accuracy of the entire project, the root mean square error (RMSE) formula was used (5):

$$RMSE_p = \sqrt{\frac{\sum_{i=1}^n (X_{Oi} - X_{GNNSi})^2 + (Y_{Oi} - Y_{GNNSi})^2 + (Z_{Oi} - Z_{GNNSi})^2}{n}} \quad (5)$$

where n is the number of reference points; X_{O_i} , Y_{O_i} , and Z_{O_i} are the X, Y, and Z coordinates that were obtained after the initial aerotriangulation; and X_{GNSS_i} , Y_{GNSS_i} , and Z_{GNSS_i} are the X, Y, and Z coordinates that were measured using a GNSS receiver in the field.

When working with germination data, we divided all the data for three years into two groups: test and verification. Several intervals were formed based on the data from the test plots. To complete this, we used Sturges' rule [47], which allowed us to optimally determine the number of intervals into which we divided the observed range.

Determining the number of groups (6):

$$n = 1 + 3.322 \lg N \quad (6)$$

where N is the total number of observations of the magnitude and \lg is the decimal logarithm.

Interval step (7):

$$h = \frac{x_{max} - x_{min}}{n} \quad (7)$$

where X_{max} and X_{min} are the maximum and minimum values in the sample, and n is the number of groups.

To assess the accuracy, the average absolute percentage error (average absolute percentage error) of MAPE (8) was calculated:

$$MAPE = \frac{\sum_{t=1}^n \frac{T_t - P_t}{T_t}}{n} \times 100 \quad (8)$$

where T_t is the received data, P_t is the predicted data, and n is the number of plots.

Forecast accuracy in percentage display (9):

$$P = 1 - MAPE \quad (9)$$

Based on the calculated ranges, software was written for automatic evaluation of the germination of soybean crops. The program was written in the C# programming language. The input data included the contours of the plots (file type .geojson), the average values of vegetation indices for each plot (file type .xlsx), ranges for soybean germination (file type .docx), and a vegetation index map (file type .geotiff) (Figure 4). The output data contained a visual display of the germination level of soybean plots (germination map) and a quantitative calculation of plots by germination level.

In general, the methodology of this study was divided into two types of research; namely, the collection of ground data and aerial data, which took place in every researched year (2020–2022) (Figure 5). As part of the aerial research, aerial photography data were collected and processed, as well as the calculation of the average value of the vegetation indices NDVI, NDRE, and ClGreen for each of the studied plots. In the ground-based studies, germination was evaluated and the data were converted into a percentage. After calculating the germination ranges based on ground and aerial data, the results obtained were evaluated using MAPE. In the end, the developed program was used to create an overview layer of visualization of the germination level of breeding plots. The program evaluated each plot using three VIs. If all three VIs showed the same germination level, then this level was assigned to the plot. If two of the three VIs showed one germination level and the third VI showed another, then the plot was assigned a germination level relative to the two indices. If all indices indicated different germination levels, then the plot was assigned an average germination level between them. Such an algorithm was necessary to avoid errors when evaluating plots using one index; for example, if a plot had high NDVI and ClGreen values but low NDRE values, the plot was assigned a germination level corresponding to the NDVI and ClGreen values, and the NDRE values were considered only if they were two or three levels lower.

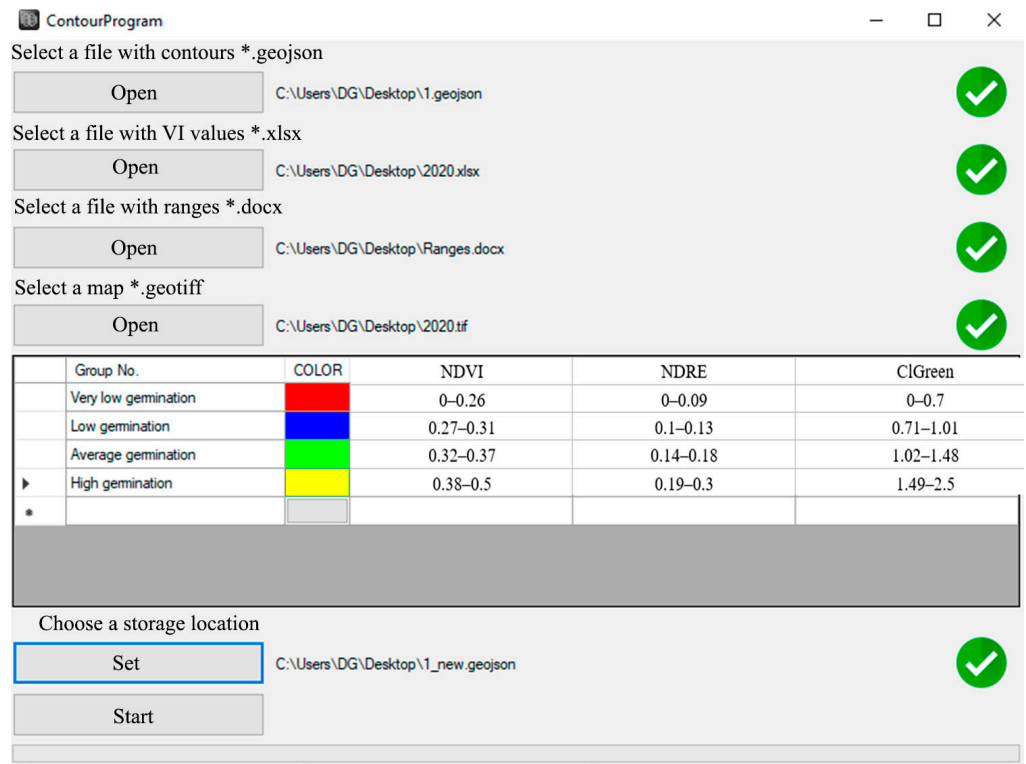


Figure 4. The initial screen of the program.

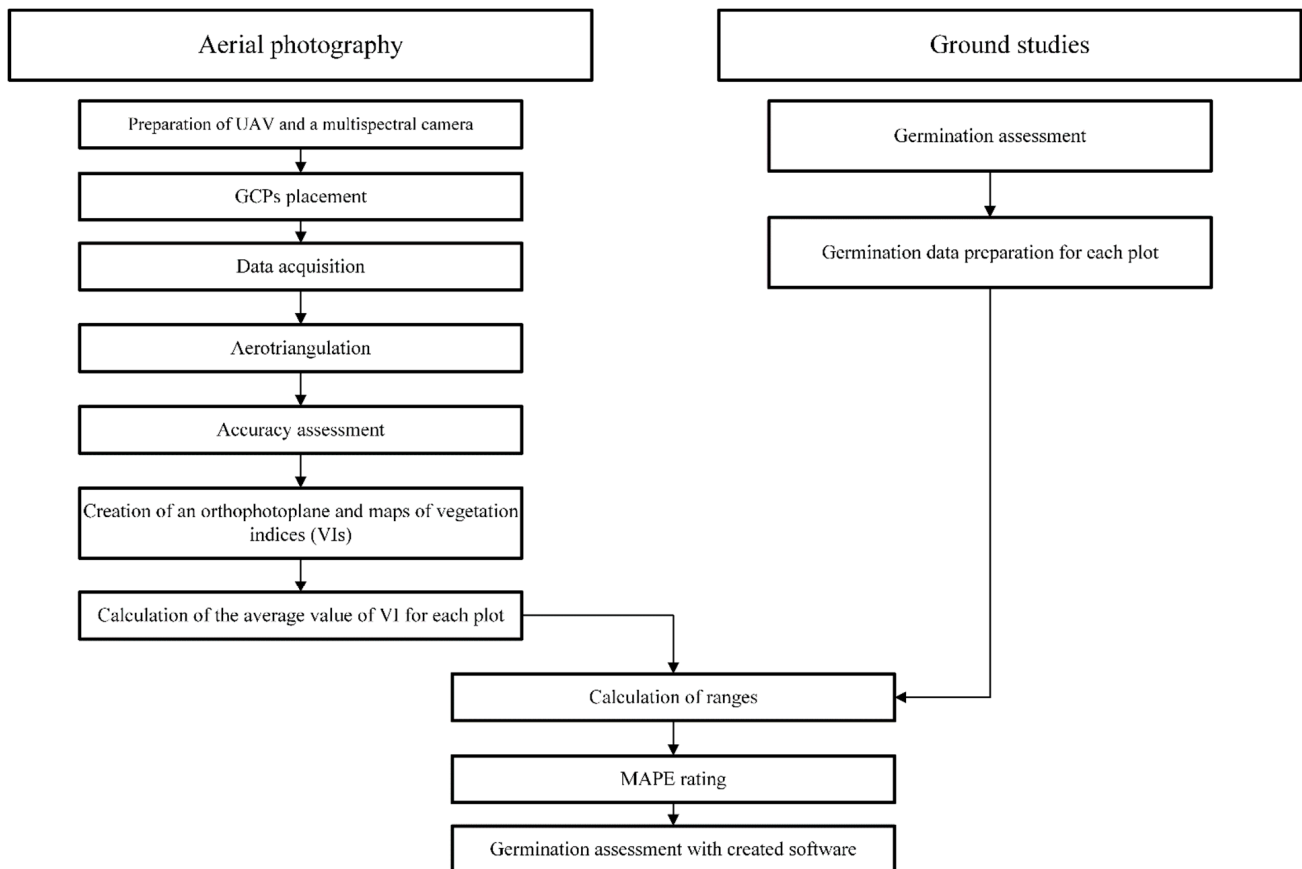


Figure 5. Overall methodology workflow.

3. Results

On 11 June 2020, 13 June 2021, and 14 June 2022, monitoring was carried out with a UAV and a multispectral camera. Flight parameters for each year are presented in Table 1. The altitude, speed of flight, and overlap of images did not change throughout the study.

Table 1. Flight parameters.

Parameter	2020	2021	2022
Flight date	11 June	13 June	14 June
Flight time of day	12:00	13:00	12:00
Flight altitude, m	120	120	120
Survey time	5 m 12 s	8 m 23 s	6 m 20 s
Transverse/longitudinal overlap RGB (MSD), %	75/85 (75/75)	75/85 (75/75)	75/85 (75/75)
Flight speed, m/s	7	7	7
Ground sampling distance (GSD) RGB/MSD, cm/px	3.39/5.22	3.48/5.9	3.28/5.37
Flying area, ha	2	4.5	3.2
Number of images RGB/MSD	46/504	103/1141	80/822

RGB and MSD images were collected during each flight. During the three years of the study, 2696 images were collected. The volume of raw data was 14,163 Mb. The total data volume of the current study was 32,253 Mb [48]. The total amount of data considered the volume of raw data, the size of PIX4Dmapper software projects and the created digital maps (Table 2).

Table 2. Data parameters.

Parameter	2020	2021	2022
Raw data size RGB/MSD, Mb	380/2500	852/5650	691/4090
PIX4Dmapper project size RGB/MSD, Mb	1290/2100	2860/4680	2150/3510
Maps data size RGB/MSD, Mb	131/177	290/390	218/294
Total data storage, Mb	6578	14,722	10,953

After the flight, an orthophotoplane was created, and the vegetation indices NDVI, NDRE, and ClGreen were calculated (Figure 6). The accuracy of the projects was evaluated for RGB and MSD. There were six projects. The RMSEp calculation was performed after the initial aerotriangulation and marking of all GCPs. The project error did not exceed three centimeters for all projects according to the PIX4Dmapper Report.

After calculating the average value of vegetation indices and the percentage of germination for each of the plots, a correlation analysis of ground and air data was carried out. Correlation analysis of the obtained germination data and values of vegetation indices (Figure 7):

- for germination and NDVI, $r = 0.72$;
- for germination and NDRE, $r = 0.70$;
- for germination and ClGreen, $r = 0.75$.

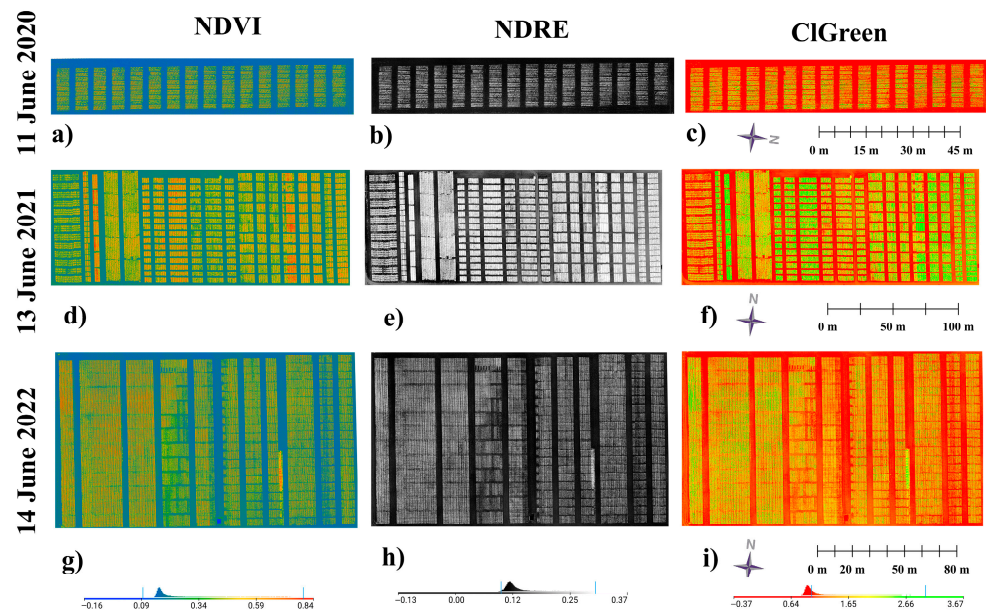


Figure 6. Digital maps of NDVI (a,d,g), NDRE (b,e,h), and ClGreen (c,f,i) from 11 June 2020 (a–c), 13 June 2021 (d–f), and 14 June 2022 (g–i).

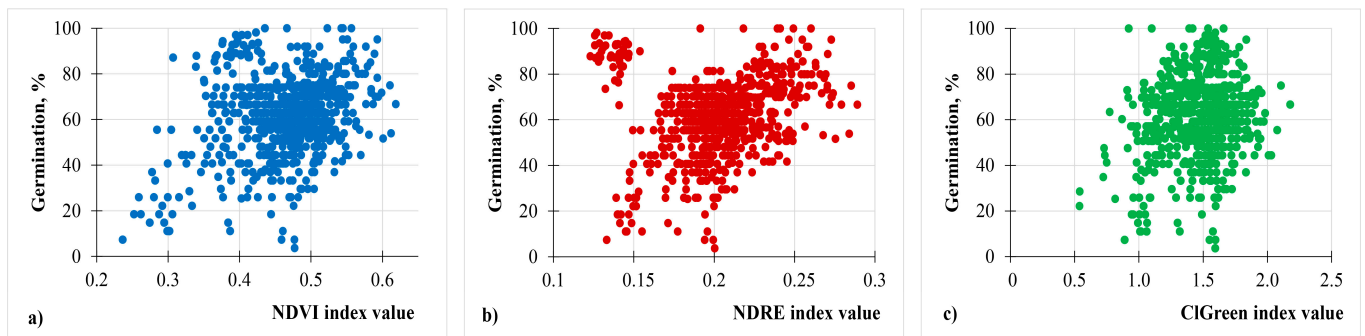


Figure 7. The ratio of germination and average values of vegetation indices (a) NDVI; (b) NDRE; (c) ClGreen.

The obtained indicators show the presence of a positive relationship of an average degree between the data.

As a result, 1460 plots were divided into two groups: test and verification. The test group contained 744 plots and the verification group contained 716 plots. For the test plots, the number of germination groups according to the Sturges' rule was (10):

$$n = 1 + 3.322lg744 = 10.5394 \tag{10}$$

The interval step was (11):

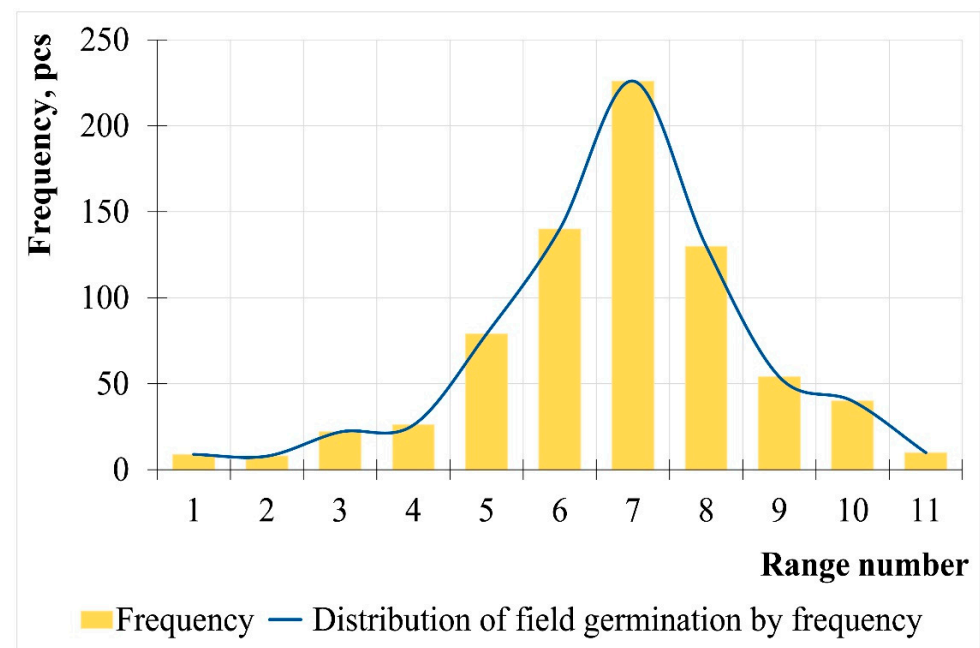
$$h = \frac{100 - 3.7}{10.5394} = 9.14 \tag{11}$$

Ranges for eleven groups of field germination were obtained (Table 3), where the first group was the lowest germination, and the eleventh group was the highest germination. For low germination, the minimum value is assumed to be 0%, and the maximum value for high germination is 100%.

Table 3. Germination ranges of soybean plants.

Group No.	Range
1	0–12.84
2	12.85–21.99
3	22–31.14
4	31.15–40.29
5	40.3–49.44
6	49.45–58.59
7	58.6–67.74
8	67.75–76.89
9	76.9–86.04
10	86.05–95.19
11	95.2–100

There is a frequency of distribution of field germination in the eleven groups shown in Figure 8. The main distribution falls in groups 6–8. When assessing the degree of asymmetry, an insignificant ($p = 0.05$) left-sided asymmetry was revealed. In this case, the deviation from the normal distribution was considered insignificant, with SEx (mean square error of the kurtosis coefficient) < 3 (SEx = 0.768).

**Figure 8.** Distribution of field germination of test plots of soybean crops by frequency.

To simplify the assessment of field germination, a grouping was created with the following ranges:

- Group 1 (1): very low germination: 0–12.84;
- Group 2 (2–3): low germination: 12.85–31.14;
- Group 3 (4–6): average germination: 31.15–58.59;
- Group 4 (7–11): high germination: 58.6–100.

Of the 744 plots, 9 plots had very low germination; 30 plots had low germination; 245 plots had average germination; and 460 plots had high germination. In accordance with Section 2.4, the Sturges' rule was applied to identify ranges of vegetation indices (Table 4).

Table 4. Ratio of germination ranges and values of vegetation indices.

Group No.	Germination Range, %	NDVI Range	NDRE Range	CIGreen Range
Very low germination	0–12.84	0–0.26	0–0.09	0–0.7
Low germination	12.85–31.14	0.27–0.31	0.1–0.13	0.71–1.01
Average germination	31.15–58.59	0.32–0.37	0.14–0.18	1.02–1.48
High germination	58.6–100	0.38–0.5	0.19–0.3	1.49–2.5

We assigned a value for the data of each of the groups for ground and air research: very low germination: 0; low germination: 1; average germination: 2; and high germination: 3. Indicators for 84 validation plots for 2020, 184 plots for 2021, and 448 plots for 2022 were also assigned values. The MAPE error showed the accuracy of the obtained results (Table 5). The final value of MAPE was calculated under the condition that the average values of vegetation indices fell into at least two of the three ranges, and then the appropriate germination level was assigned. If this condition was not met, then the germination level was assigned below the one under consideration.

Table 5. The accuracy of the obtained data.

Vegetation Index	NDVI	NDRE	CIGreen	Overall
Accuracy of 84 test plots in 2020, %	96.43	82.94	94.44	95.24
Accuracy of 184 test plots in 2021, %	94.93	87.86	95.05	96.39
Accuracy of 448 test plots in 2022, %	97.02	89.25	96.5	94.02

The percentage of error did not exceed 10% for the vegetation indices NDVI and CIGreen, which indicates a high accuracy of the data obtained. For the NDRE vegetation index, the error percentage was higher and reached 18%. The smallest error of 2.98% was detected in 2022 for ranges of NDVI values. The final values of MAPE for three years did not exceed 10%.

Germination maps were created for the 2020–2022 years using software for automatic evaluation of the germination of soybean crops (Figure 9). Based on the results of the program, the number of plots for each of the germination levels for three years for verification plots was calculated (Table 6). Evaluation of the accuracy of the software was carried out relative to the data obtained by breeders. The maximum error of the software did not exceed 10% for each of the germination levels.

Table 6. Germination assessment of soybean plots.

Group No.	Year								
	2020			2021			2022		
	Breeders' Assessment	Software Assessment	Error, % *	Breeders' Assessment	Software Assessment	Error, % *	Breeders' Assessment	Software Assessment	Error, % *
High germination	72	70	2.4	169	158	6.0	421	383	8.5
Average germination	9	12	−3.6	12	18	−3.3	23	64	−9.2
Low germination	2	2	0.0	2	5	−1.6	2	1	0.2
Very low germination	1	0	1.2	1	3	−1.1	2	0	0.4

* $E = \frac{A_S - A_B}{n} \times 100$ E-Error, %; A_S —Software assessment; A_B —Breeders' assessment.

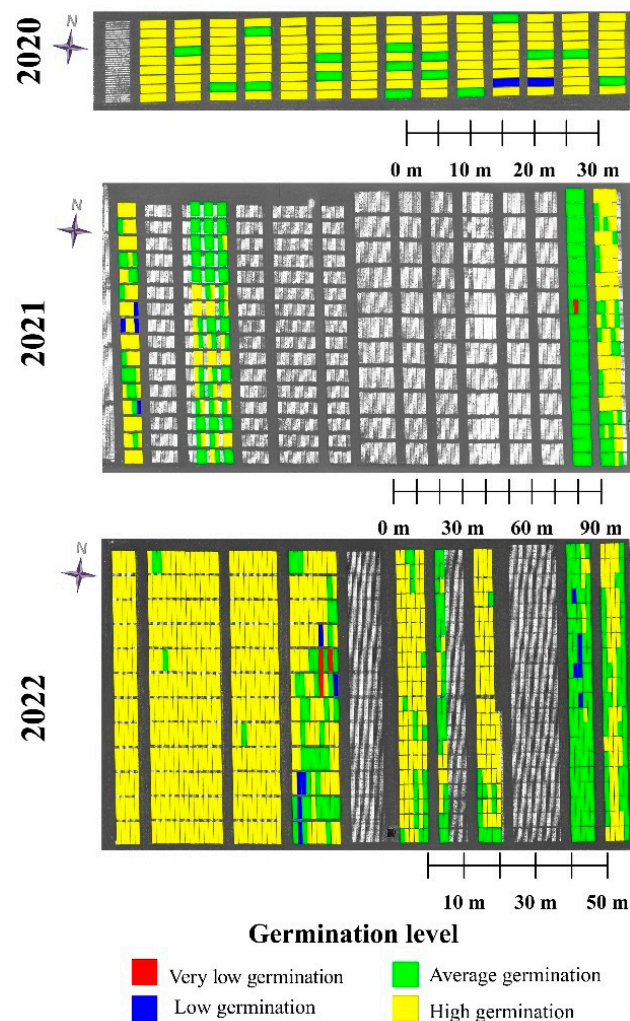


Figure 9. Germination maps for soybean plots in 2020, 2021, and 2022.

4. Discussion

As a result of the three-year study, vegetation maps of three vegetation indices (NDVI, NDRE, and ClGreen) of soybean breeding crops in the full germination phase were created. The project error along the X, Y, and Z axes did not exceed 3 cm ($RMSE_p < 3$ cm). This indicated a high point in the construction of digital maps (orthophotoplane and vegetation maps) [49,50].

Comparative analysis of field germination using the method of vegetation indices and by conducting ground measurements showed their general patterns. Thus, the use of the values of the vegetation indices NDVI, NDRE, and ClGreen revealed a correlation with the ground assessment of field germination (Table 2). The correlation coefficients here were quite close and amounted to $r = 0.70$ – 0.75 , which may indicate the applicability in the calculations of each of the presented vegetation indices. The average absolute percentage error has been calculated in many studies on the use of UAVs in agriculture [51–59]. Studies with a high level of accuracy consider MAPE values up to 15% [52,56–59]. In the current study, the MAPE values did not exceed 10% for two vegetation indices (NDVI, ClGreen) and was 18% for one vegetation index (NDRE). The overall MAPE for every year did not exceed 10%, which indicated high accuracy of the results of the germination assessment using multispectral data from the UAV. The presence of an error of approximately 10% was possible due to many factors, for example, the use of a breeding seeder without an accurate seeding system [60], varietal characteristics, soil, and climatic conditions.

The developed software allowed us to evaluate the germination of soybean crops according to three vegetation indices. The greatest errors were observed for the germination levels of average and high germination. Under favorable ecological and climatic conditions, the largest number of soybean plots had an average or high germination rate. The difficulty in assessing germination lies in finding the correct ranges for each of the germination levels. Despite all the difficulties, the software showed high accuracy, providing an error rate of less than 10% for each of the groups.

To be able to repeat the experiment, aerial and ground surveys were carried out every year only during the full germination phase. Aerial photography was carried out according to the recommendations for collecting multispectral data (<https://support.micasense.com/hc/en-us/articles/224893167-Best-Practices-Collecting-Data-with-MicaSense-Sensors>, accessed on 25 April 2020). The calibration panel and DLS 2 for a MicaSense Altum were used. We did not set the task to compare the numerical indicators of field germination with the values of vegetation indices; therefore, the study used the percentage values of field germination relative to the seeding rate. The germination rate was influenced by weather conditions at the time of seed germination, including air temperature and precipitation, regardless of the location of sowing.

The size of the breeding plots was dictated by the requirements for the methodology of field experience. This technique is standardized in the Russian Federation [35–37]. The experience shown in this article is an additional study of the material used for breeding work. The statistical power of this study was achieved by combining small plots into larger groups. At this phase of plant development, the marginal effect was insignificant, and the entire selection of breeding plots reflected the properties of the general population of soybean plants regardless of variety, such as the place of sowing or other environmental factors.

The advantages of the survey of breeding crops with the help of UAVs were high efficiency and productivity; however, the reliability of the information received and the ability to assess it in the field was difficult. The method proposed in this study for assessing the field germination of breeding plots was considered an additional tool for the breeder to assess the development of new varieties. In the future study of additional vegetation indices, special attention will be paid to the vegetation indices calculated on the blue channel. Additional research is needed to develop a new methodology as the breeder's main tool for assessing the field germination of soybean breeding seedlings.

5. Conclusions

As a result of this study, the field germination data of soybean plants for three years (1460 plots) and the average values of the vegetation indices NDVI, NDRE, and ClGreen were analyzed. The correlation coefficients of vegetation indices and ground-based assessment ($r = 0.70\text{--}0.75$) indicated an average positive relationship between multispectral and ground-based studies. The ranges of field germination (very low, low, average, and high field germination) were calculated for the ground data and the vegetation indices NDVI, NDRE, and ClGreen. The values of the average absolute percentage error for the test plots in 2020–2022 did not exceed 10% for the NDVI and ClGreen indices, or 18% for the NDRE, and the overall MAPE was less than 10%, indicating a high level of accuracy of the obtained germination ranges. The ratios of germination ranges and values of vegetation indices were revealed, forming the basis of the developed software for assessing soybean germination. The percentage of software errors for each germination level did not exceed 10%. This software will serve as a tool for assessing the field germination of soybean breeding plots in 2023–2024 in the fields of the FGBNU FNC ZBK.

Thus, the evaluation of field germination of soybean breeding crops using the vegetation indices NDVI, NDRE, and ClGreen can be an independent method. The use of this method makes it possible to evaluate the field germination of a large number of experimental plots and the influence of genotype and various elements of agrotechnology on this indicator.

Author Contributions: Data curation, V.P. and P.Y.; Formal analysis, V.P., A.P., M.L. and E.G. (Ekaterina Golovina); Funding acquisition, D.E.K.; Investigation, Y.L., N.Y.R. and V.R.; Methodology, R.K., A.P., N.Z., E.G. (Elena Gureeva) and V.R.; Project administration, N.Z.; Resources, R.K. and P.Y.; Software, E.G. (Ekaterina Golovina); Validation, P.Y. and A.M.A.; Visualization, Y.L. and M.L.; Writing—original draft, R.K., N.Y.R., E.G. (Elena Gureeva) and V.R.; Writing—review and editing, A.M.A. All authors have read and agreed to the published version of the manuscript.

Funding: This research received no external funding.

Institutional Review Board Statement: Not applicable.

Informed Consent Statement: Not applicable.

Data Availability Statement: Not applicable.

Acknowledgments: The authors would like to thank the Federal Scientific Agroengineering Center VIM for funding the field survey and remote sensing work. The authors would like to thank the Federal Scientific Center of Legumes and Groat Crops, Russia, for supervising this work and for sample analysis. «This publication has been supported by the RUDN University Scientific Projects Grant System, project № <202724-2-000>». The authors would like to extend their sincere appreciation to the National Authority of Remote Sensing and Space Science (NARSS), Cairo, Egypt.

Conflicts of Interest: The authors declare no conflict of interest.

References

- Manylova, O.V.; Zharkova, S.V. Field Germination and Preservation of Soybean Plants for Harvesting, Depending on the Elements of Agricultural Technology. *Int. J. Humanit. Nat. Sci.* **2021**, *12*-3, 41–43. [CrossRef]
- Švubová, R.; Slováková, L.; Holubová, L.; Rovňanová, D.; Gálová, E.; Tomeková, J. Evaluation of the Impact of Cold Atmospheric Pressure Plasma on Soybean Seed Germination. *Plants* **2021**, *10*, 177. [CrossRef] [PubMed]
- Nemenushchaya, L.; Konovalenko, L.; Shchegolikhina, T. Development of Russian selection and seed production under the Federal scientific and technical program for agricultural development. *E3S Web Conf.* **2020**, *164*, 06014. [CrossRef]
- Mamlic, Z.; Maksimovic, I.; Canak, P.; Mamlic, G.; Djukic, V.; Vasiljevic, S.; Dozet, G. The Use of Electrostatic Field to Improve Soybean Seed Germination in Organic Production. *Agronomy* **2021**, *11*, 1473. [CrossRef]
- Federal Law of the Russian Federation “On Seed Production” dated December 17, 1997 No. 149 FZ (with amendments and additions). Available online: <http://ivo.garant.ru/#/document/12106441/paragraph/18117:0> (accessed on 30 March 2022).
- Nagorny, V.D.; Lyashko, M.U. *Biology and Agricultural Engineering of Soybeans*; Biblio-Globe: Moscow, Russia, 2018; 418p.
- Dorokhov, A.S.; Evdokimova, O.V.; Bolsheva, K.K. Overview of the world soybean market. *Innov. Agric.* **2018**, *4*, 237–246.
- Akhalaya, B.K.; Shogenov, Y.K.; Starovoitov, S.I.; Tsench, Y.S. Three-Section Soil Processing Unit with Universal Replaceable Working Units. *Bull. Kazan State Agrar. Univ.* **2019**, *3*, 92–95. [CrossRef]
- Torikov, V.E.; Belchenko, S.A.; Dronov, I.Y.; Moiseenko, I.Y.; Zaycheva, O.A. *Soybeans of the Northern Ecotype in Intensive Agriculture*; Bryansk GAU: Bryansk, Russia, 2019; 284p.
- Barnakov, N.V. *Scientific Foundations of Seed Production of Grain Crops*; The Science: Novosibirsk, Russia, 1982; 328p.
- Lamichhane, J.R.; Constantin, J.; Schoving, C.; Maury, P.; Debaeke, P.; Aubertot, J.N.; Dürr, C. Analysis of soybean germination, emergence, and prediction of a possible northward establishment of the crop under climate change. *Eur. J. Agron.* **2020**, *113*, 125972. [CrossRef]
- Lobachevsky, Y.P.; Dorokhov, A.S. Promising scientific and technical projects in the field of mechanization and robotization of agriculture. In *Formation of a Single Scientific and Technological Space of the Union State: Problems, Prospects, Innovations*; Center for System Analysis and Strategic Studies of the National Academy of Sciences of Belarus: Minsk, Belarus, 2017; pp. 333–343.
- Mazitov, N.K.; Shogenov, Y.K.; Tsench, Y.S. Agricultural machinery: Solutions and prospects. *Bull. VIESKH* **2018**, *3*, 94–100.
- Chen, Y.; Weng, Q.; Tang, L.; Wang, L.; Xing, H.; Liu, Q. Developing an intelligent cloud attention network to support global urban green spaces mapping. *ISPRS J. Photogramm. Remote Sens.* **2023**, *198*, 197–209. [CrossRef]
- Natarajan, S.; Basnayake, J.; Wei, X.; Lakshmanan, P. High-throughput phenotyping of indirect traits for early-stage selection in sugarcane breeding. *Remote Sens.* **2019**, *11*, 2952. [CrossRef]
- Ge, H.; Ma, F.; Li, Z.; Du, C. Grain Yield estimation in rice breeding using phenological data and vegetation indices derived from UAV images. *Agronomy* **2021**, *11*, 2439. [CrossRef]
- Prey, L.; Hanemann, A.; Ramgraber, L.; Seidl-Schulz, J.; Noack, P.O. UAV-Based estimation of grain yield for plant breeding: Applied strategies for optimizing the use of sensors, vegetation indices, growth stages, and machine learning algorithms. *Remote Sens.* **2022**, *14*, 6345. [CrossRef]
- Oehme, L.H.; Reineke, A.-J.; Weiß, T.M.; Würschum, T.; He, X.; Müller, J. Remote sensing of maize plant height at different growth stages using uav-based digital surface models (DSM). *Agronomy* **2022**, *12*, 958. [CrossRef]
- Zhou, J.; Yungbluth, D.; Vong, C.N.; Scaboo, A.; Zhou, J. Estimation of the maturity date of soybean breeding lines using uav-based multispectral imagery. *Remote Sens.* **2019**, *11*, 2075. [CrossRef]

20. Elfanah, A.M.S.; Darwish, M.A.; Selim, A.I.; Shabana, M.M.A.; Elmoselhy, O.M.A.; Khedr, R.A.; Ali, A.M.; Abdelhamid, M.T. Spectral reflectance indices' performance to identify seawater salinity tolerance in bread wheat genotypes using genotype by yield*trait biplot approach. *Agronomy* **2023**, *13*, 353. [[CrossRef](#)]
21. Deng, L.; Mao, Z.; Li, X.; Hu, Z.; Duan, F.; Yan, Y. UAV-based Multispectral Remote Sensing for Precision Agriculture: A Comparison between Different Cameras. *ISPRS J. Photogramm. Remote Sens.* **2018**, *146*, 124–136. [[CrossRef](#)]
22. Di Gennaro, S.F.; Toscano, P.; Gatti, M.; Poni, S.; Berton, A.; Matese, A. Spectral Comparison of UAV-Based Hyper and Multispectral Cameras for Precision Viticulture. *Remote Sens.* **2022**, *14*, 449. [[CrossRef](#)]
23. Navia, J.; Mondragon, I.; Patino, D.; Colorado, J. Multispectral Mapping in Agriculture: Terrain Mosaic Using an Autonomous Quadcopter UAV. In Proceedings of the International Conference on Unmanned Aircraft Systems (ICUAS), Arlington, VA, USA, 7–10 June 2016; pp. 1351–1358. [[CrossRef](#)]
24. Randelović, P.; Đorđević, V.; Milić, S.; Balešević-Tubić, S.; Petrović, K.; Miladinović, J.; Đukić, V. Prediction of Soybean Plant Density Using a Machine Learning Model and Vegetation Indices Extracted from RGB Images Taken with a UAV. *Agronomy* **2020**, *10*, 1108. [[CrossRef](#)]
25. Yue, J.; Feng, H.; Tian, Q.; Zhou, C. A robust spectral angle index for remotely assessing soybean canopy chlorophyll content in different growing stages. *Plant Methods* **2020**, *16*, 104. [[CrossRef](#)]
26. Kurbanov, R.K.; Zakharova, N.I. Application of Vegetation Indexes to Assess the Condition of Crops. *Agric. Mach. Technol.* **2020**, *14*, 4–11. [[CrossRef](#)]
27. Zhou, J.; Beche, E.; Vieira, C.C.; Yungbluth, D.; Zhou, J.F.; Scaboo, A.; Chen, P.Y. Improve Soybean Variety Selection Accuracy Using UAV-Based High-Throughput Phenotyping Technology. *Front. Plant Sci.* **2022**, *12*, 768742. [[CrossRef](#)] [[PubMed](#)]
28. Zhang, X.; Zhao, J.; Yang, G.; Liu, J.; Cao, J.; Li, C.; Zhao, X.; Gai, J. Establishment of Plot-Yield Prediction Models in Soybean Breeding Programs Using UAV-Based Hyperspectral Remote Sensing. *Remote Sens.* **2019**, *11*, 2752. [[CrossRef](#)]
29. Da Silva, E.E.; Baio, F.H.R.; Teodoro, L.P.R.; da Silva Junior, C.A.; Borges, R.S.; Teodoro, P.E. UAV-multispectral and vegetation indices in soybean grain yield prediction based on in situ observation. *Remote Sens. Appl. Soc. Environ.* **2020**, *18*, 100318. [[CrossRef](#)]
30. Belyshkina, M.; Zagoruiko, M.; Mironov, D.; Bashmakov, I.; Rybalkin, D.; Romanovskaya, A. The Study of Possible Soybean Introduction into New Cultivation Regions Based on the Climate Change Analysis and the Agro-Ecological Testing of the Varieties. *Agronomy* **2023**, *13*, 610. [[CrossRef](#)]
31. Zhou, J.; Mou, H.; Zhou, J.; Md Liakat, A.; Ye, H.; Chen, P.; Nguyen, H.T. Qualification of Soybean Responses to Flooding Stress Using UAV-Based Imagery and Deep Learning. *Plant Phenomics* **2021**, *2021*, 9892570. [[CrossRef](#)] [[PubMed](#)]
32. Zhou, J.; Zhou, J.; Ye, H.; Ali, M.L.; Nguyen, H.T.; Chen, P. Classification of soybean leaf wilting due to drought stress using UAV-based imagery. *Comput. Electron. Agric.* **2020**, *175*, 105576. [[CrossRef](#)]
33. Etienne, A.; Saraswat, D. Machine learning approaches to automate weed detection by UAV based sensors. In *Proceedings of the SPIE 11008, Autonomous Air and Ground Sensing Systems for Agricultural Optimization and Phenotyping IV*; SPIE: Baltimore, MD, USA, 2019; Volume 110080R. [[CrossRef](#)]
34. Kurbanov, R.K.; Zakharova, N.I. Justification and selection of vegetation indices to determine the early soybeans readiness for harvesting. In Proceedings of the 14th International Scientific and Practical Conference on State and Prospects for the Development of Agribusiness, Interagromash, Rostov-on-Don, Russia, 24–26 February 2021; p. 01008.
35. Dospikhov, B.A. *Methodology of Field Experience (with the Basics of Statistical Processing of Research Results)*, 5th ed.; Agroprom Izdat: Moscow, Russia, 1985; 351p.
36. Federal State Budgetary Institution. "State Commission of the Russian Federation for Testing and Protection of Breeding Achievements" *Methodology of State Variety Testing of Agricultural Crops*; General Part; Federal State Budgetary Institution: Moscow, Russia, 2019; 329p.
37. GOST R 52325-2005; Seeds of Agricultural Plants. Varietal and Sowing Qualities. General Technical Conditions. Standartinform: Moscow, Russia, 2005.
38. Shchelko, L.G.; Sedova, T.S.; Korneychuk, V.A. *The International Classifier of the CMEA Genus Glycine Willd*; VIR: Leningrad, Russia, 1990; 38p.
39. Kurbanov, R.K.; Zakharova, N.I.; Sidorenko, V.; Vilyunov, S. The Use of Vegetation Indices in Comparison to Traditional Methods for Assessing Overwintering of Grain Crops. *Lect. Notes Data Eng. Commun. Technol.* **2022**, *119*, 52–64.
40. Barnhart, I.; Demarco, P.; Prasad, P.V.; Mayor, L.; Jugulam, M.; Ciampitti, I.A. High-resolution unmanned aircraft systems imagery for stay-green characterization in grain sorghum (*Sorghum bicolor* L.). *J. Appl. Remote Sens.* **2021**, *15*, 044501. [[CrossRef](#)]
41. Daugela, I.; Visockiene, J.S.; Kumpiene, J. Detection and analysis of methane emissions from a landfill using unmanned aerial drone systems and semiconductor sensors. *Detritus* **2020**, *10*, 127–138. [[CrossRef](#)]
42. Bawa, A.; Samanta, S.; KHimanshu, S.; Singh, J.; Kim, J.J.; Zhang, T.; Chang, A.; Jung, J.; De-Laune, P.; Bordovsky, J.; et al. A support vector machine and image processing based approach for counting open cotton bolls and estimating lint yield from UAV imagery. *Smart Agric. Technol.* **2023**, *3*, 100140. [[CrossRef](#)]
43. Xiao, D.; Pan, Y.; Feng, J.; Yin, J.; Liu, Y.; He, L. Remote sensing detection algorithm for apple fire blight based on UAV multispectral image. *Comput. Electron. Agric.* **2022**, *199*, 107137. [[CrossRef](#)]
44. Trevisan, R.; Pérez, O.; Schmitz, N.; Diers, B.; Martin, N. High-throughput phenotyping of soybean maturity using time series uav imagery and convolutional neural networks. *Remote Sens.* **2020**, *12*, 3617. [[CrossRef](#)]

45. Wang, N.; Guo, Y.; Wei, X.; Zhou, M.; Wang, H.; Bai, Y. UAV-based remote sensing using visible and multispectral indices for the estimation of vegetation cover in an oasis of a desert. *Ecol. Indic.* **2022**, *41*, 109155. [[CrossRef](#)]
46. Marin, D.B.; Ferraz, G.A.; Santana, L.S.; Barbosa, B.D.S.; Barata, R.A.P.; Osco, L.P.; Ramos, A.P.M.; Guimarães, P.H.S. Detecting coffee leaf rust with UAV-based vegetation indices and decision tree machine learning models. *Comput. Electron. Agric.* **2021**, *190*, 106476. [[CrossRef](#)]
47. David, S. Sturges' rule. *Wiley Interdiscip. Rev. Comput. Stat.* **2009**, *1*, 303–306.
48. Kayad, A.; Sozzi, M.; Paraforos, D.S.; Rodrigues, F.A.; Cohen, Y.; Fountas, S.; Francisco, M.-J.; Pezzuolo, A.; Grigolato, S.; Marinello, F. How many gigabytes per hectare are available in the digital agriculture era? A digitization footprint estimation. *Comput. Electron. Agric.* **2022**, *198*, 107080. [[CrossRef](#)]
49. Santos Santana, L.; Araújo ESilva Ferraz, G.; Bedin Marin, D.; Dienevam Souza Barbosa, B.; Mendes Dos Santos, L.; Ferreira Ponciano Ferraz, P.; Conti, L.; Camiciottoli, S.; Rossi, G. Influence of flight altitude and control points in the georeferencing of images obtained by unmanned aerial vehicle. *Eur. J. Remote Sens.* **2021**, *54*, 59–71. [[CrossRef](#)]
50. Kapicioglu, H.S.; Hastaoglu, K.O.; Poyraz, F.; Gül, Y. Investigation of topographic effect in ground control point selection in UAV photogrammetry: Gaziantep/Nizip. *Int. Conf. Innov. Eng. Appl.* **2018**, 1174–1178.
51. Costa, L.; Kunwar, S.; Ampatzidis, Y.; Albrecht, U. Determining leaf nutrient concentrations in citrus trees using UAV imagery and machine learning. *Precis. Agric.* **2022**, *23*, 854–875. [[CrossRef](#)]
52. Hou, M.; Tian, F.; Ortega-Farias, S.; Riveros-Burgos, C.; Zhang, T.; Lin, A. Estimation of Crop Transpiration and Its Scale Effect Based on Ground and UAV thermal infrared remote sensing images. *Eur. J. Agron.* **2021**, *131*, 126389. [[CrossRef](#)]
53. Shaikh, Y.Y.J.; Vinay, P.; Lawal, B.; Stephen, D.T.; Deepak, G.; Debbie, S.; Hui, C.H.; Ajit, S. The Feasibility of Using a Low-Cost Near-Infrared, Sensitive, Consumer-Grade Digital Camera Mounted on a Commercial UAV to assess Bambara Groundnut Yield. *Int. J. Remote Sens.* **2022**, *43*, 393–423. [[CrossRef](#)]
54. Wang, F.; Yao, X.; Xie, L.; Zheng, J.; Xu, T. Rice Yield Estimation Based on Vegetation Index and Florescence Spectral Information from UAV Hyperspectral Remote Sensing. *Remote Sens.* **2021**, *13*, 3390. [[CrossRef](#)]
55. Koh, J.C.O.; Spangenberg, G.; Kant, S. Automated Machine Learning for High-Throughput Image-Based Plant Phenotyping. *Remote Sens.* **2021**, *13*, 858. [[CrossRef](#)]
56. Dos Santos, A.; Biesseck, B.J.G.; Latte, N.; de Lima Santos, I.C.; dos Santos, W.P.; Zanetti, R.; Zanoncio, J.C. Remote detection and measurement of leaf-cutting ant nests using deep learning and an unmanned aerial vehicle. *Comput. Electron. Agric.* **2022**, *198*, N107071. [[CrossRef](#)]
57. Zhou, J.; Lu, X.; Yang, R.; Chen, H.; Wang, Y.; Zhang, Y.; Huang, J.; Liu, F. Developing Novel Rice Yield Index Using UAV Remote Sensing Imagery Fusion Technology. *Drones* **2022**, *6*, 151. [[CrossRef](#)]
58. Combs, T.P.; Didan, K.; Dierig, D.; Jarchow, C.J.; Barreto-Muñoz, A. Estimating Productivity Measures in Guayule Using UAS Imagery and Sentinel-2 Satellite Data. *Remote Sens.* **2022**, *14*, 2867. [[CrossRef](#)]
59. Gao, M.; Yang, F.; Wei, H.; Liu, X. Individual Maize Location and Height Estimation in Field from UAV-Borne LiDAR and RGB Images. *Remote Sens.* **2022**, *14*, 2292. [[CrossRef](#)]
60. Zhao, X.G.; Chen, L.P.; Gao, Y.Y.; Yang, S.; Zhai, C.Y. Optimization Method for Accurate Positioning Seeding Based on Sowing Decision. *Int. J. Agric. Biol. Eng.* **2021**, *14*, 171–180. [[CrossRef](#)]

Disclaimer/Publisher's Note: The statements, opinions and data contained in all publications are solely those of the individual author(s) and contributor(s) and not of MDPI and/or the editor(s). MDPI and/or the editor(s) disclaim responsibility for any injury to people or property resulting from any ideas, methods, instructions or products referred to in the content.